Position and Orientation Control of Complex-Shaped Samples in Acoustic Levitation

Sundblad, Felix Alexander

IEEE
2022

Sundblad , F A , Iablonskyi , D , Holmström , A , Salmi , A & Haeggström , E 2022 , Position and Orientation Control of Complex-Shaped Samples in Acoustic Levitation . in 2022 IEEE International Ultrasonics Symposium (IUS) . IEEE , 2022 IEEE International Ultrasonics Symposium (IUS) , Venice , Italy , 10/10/2022 . https://doi.org/10.1109/IUS54386.2022.9957565

http://hdl.handle.net/10138/354153
https://doi.org/10.1109/IUS54386.2022.9957565

submittedVersion

Position and Orientation Control of Complex-Shaped Samples in Acoustic Levitation

Felix Sundblad
Electronics Research Lab.
University of Helsinki
Helsinki, Finland
felix.sundblad@helsinki.fi

Denys Iabloskyi
Electronics Research Lab.
University of Helsinki
Helsinki, Finland
denys.iablonskyi@helsinki.fi

Axi Holmström
Electronics Research Lab.
University of Helsinki
Helsinki, Finland
axi.holmstrom@helsinki.fi

Ari Salmi
Electronics Research Lab.
University of Helsinki
Helsinki, Finland
ari.salmi@helsinki.fi

Edward Hæggström
Electronics Research Lab.
University of Helsinki
Helsinki, Finland
edward.haeggstrom@helsinki.fi

***Abstract*— Controlled levitation has been limited to sub-wavelength samples with few exceptions of spheres and cubes. We demonstrate controlled airborne levitation of 2λ-sized complex-shaped objects (3D letters, X, U, T). The pressure field was tailored to a particular sample shape by arranging multiple small asymmetric acoustic traps. This allows stable locking of the object and control of its orientation and position in mid-air. The pressure field was produced with a 450-element phased array (*f* = 40kHz) featuring element-wise amplitude and phase control.**

Keywords*— *Acoustic Levitation, standing waves, ultrasonic transducers, phased arrays

I. Introduction

Acoustic levitation is the phenomenon of trapping objects of different material and shape in mid-air using acoustic waves [1]. It provides a new method for non-contact sample manipulation. Acoustic levitation can be achieved with standing sound waves [2]. The acoustic standing field is generated with a single ultrasound transducer or with an array of multiple transducers. Recent advances in acoustic levitation with phased arrays allow 3D orientation lock of sub-wavelength samples [3]. The 3D orientation control can be used to handle fragile samples and therefore has applications in industry and medicine. The applications vary from contactless 3D imaging [4] to moving electronic components [5].

Although objects larger than the wavelength have been levitated, controlled levitation has been limited to sub-wavelength sample size with few exceptions, such as spheres and cubes. Previously larger-than-wavelength sample levitation was achieved using the sample as reflector [6], a multifrequency high aperture vortex trap [7], or by direct optimization of the radiation force acting on a sphere [8]. Near-field levitation achieves larger-than-wavelength levitation in close proximity to the transducer.

We propose a method to achieve position and orientation control of larger-than-wavelength-sized complex-shaped samples. Using tailored combinations of individual asymmetric acoustic traps, we demonstrated movement and rotation of a sample along all axes in mid-air. Samples need to be rigid and contain ¼ wavelength parts that fit inside the asymmetric acoustic traps. With our new method it is possible to manipulate 2 cm long letters, with respect to orientation and position, in six degrees of freedom, Fig 1.

II. Materials and Methods

A. Theorethical background

The particle can be suspended in air against gravity with the acoustic radiation force [1]. This force can be estimated using the Gor'kov potential [9]. However, this potential only applies to rigid samples much smaller than the wavelength. For bigger objects a closed form expression for force calculation exists only for spherical samples [10]. Hence to estimate the pressure field acting on larger-than-wavelength-sized complex shapes, a method like the Finite Element Method (FEM) is needed in order to calculate the acoustic pressure that acts on the sample surface. The general expression to estimate radiation forces acting on a rigid object of any shape was presented in [11]. To first order, the time-averaged harmonic pressure $\langle p_1 \rangle$ is zero. Following the derivation in [11], the second order pressure can be expressed in terms of p_1:

$$\langle p_2 \rangle = \frac{1}{2\rho_0 c_0^2} \langle p_1^2 \rangle - \frac{\rho_0}{2} \langle \boldsymbol{u_1} - \boldsymbol{u_2} \rangle, \quad (1)$$

where the particle velocity of the wave $u_1=\nabla p_1/(i\rho\omega)$, p is pressure and ρ is the density of the medium. According to perturbation theory ρ_0 is constant density. The lower indices indicate first and second harmonics of the field and $p_1=p_1^{in}+p_1^{sc}$ (incident and scattered fields). The radiation force acting on a levitating object is defined as an integral of the pressure acting on a surface:

$$\boldsymbol{F}_{rad} = -\int_{S_0} \langle \boldsymbol{p_2} \rangle \, \boldsymbol{n} \, dS, \quad (2)$$

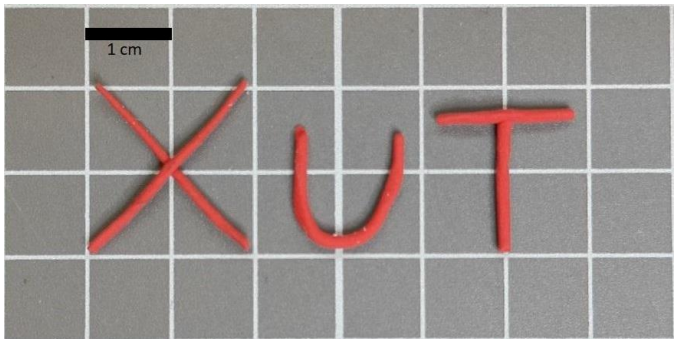

Fig. 1. Foam clay letters.

B. *Phased array levitator*

The pressure field was generated using 450 ultrasonic transducers (Multicomp MCUST10P40B07RO) arranged into two dome-shaped arrays of 15 cm diameter being 5 cm apart, with central frequency of 40 kHz ($\lambda \approx 0.9$ cm). The total complex pressure at the point $\boldsymbol{r}$ is a sum of the pressure-wave contributions from the individual transducers:

$$P(\vec{r}) = \sum_n p_n e^{i\varphi_n} e^{i\boldsymbol{k}(\boldsymbol{r}_n - \boldsymbol{r})}, \quad (3)$$

where each transducer's phase and amplitude can be calculated with a pseudo-inverse method (section C.), $\boldsymbol{k}$ is the wave number vector, p_n is the pressure amplitude of a single transducer at the calibration point, r_n is the transducer location, φ_n is the activation phase, and φ_n is the transducer's phase offset that are obtained from calibration. Calculated phases and amplitudes are sent to FPGAs, which generate the individual square signal for each narrowband transducer. The signals are amplified with level-shifters and the phase of the single transducer can be adjusted with an accuracy of $\pi/50$ [7].

C. *Asymmetric multi trap*

Orientation-locking asymmetric traps employ two independent and perpendicular standing waves of different amplitude. These perpendicular waves are phase shifted by $\pi/2$ from each other to eliminate interference. Asymmetric traps at locations $\{\boldsymbol{r}_k\}$ are created by setting the total pressure (3) to zero and by aligning its pressure gradient along the z- and x-axes:

$$P(r_j) = 0, \quad (4)$$

$$\vec{\nabla} P(\vec{r}_j) = A_j(\boldsymbol{e_z} + \alpha_j e^{i\pi/2}\boldsymbol{e_x}), \quad (5)$$

where α_k is the asymmetry parameter that represents the amplitude ratio between the horizontal and vertical standing waves, A_k is the pressure gradient amplitude. Considering (3), the left-hand side of (5) becomes $\nabla P = i\boldsymbol{k}P$. The activation function of each transducer $\{p_n,\varphi_n\}$, can be obtained by solving the linear (4) and (5). However, the solution is not unique, because the number of unknown parameters $\{p_n,\varphi_n\}$ exceeds the number of equations (4 x number of asymmetric traps). Thus, we employ a method that minimizes the total power ($\sum_n p_n^2$), here singular value decomposition (SVD).

Using a single asymmetric acoustic trap, sub-wavelength objects can be locked in mid-air [3]. To move and rotate one larger-than-wavelength-sized sample, we need to use asymmetric multi-traps, Fig. 2. The asymmetric multi-trap is a combination of individual asymmetric traps, which is tailored to the sample shape by adjusting the position and orientation of the individual asymmetric traps. The movement and rotation of the sample can then be achieved with synchronous movement and rotation of individual asymmetric traps. This was realized by changing the location and orientation of the asymmetric traps using the Euler angles convention.

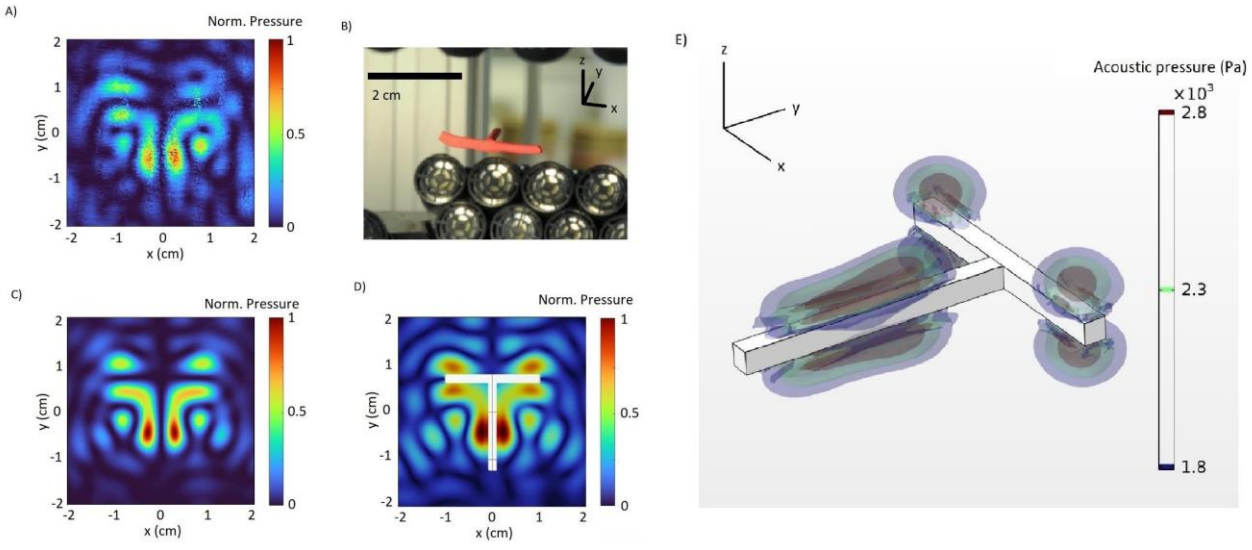

Fig. 2. A) experimentally measured pressure field normalized to highest point in the xy-plane, B) image of levitated letter 'T', C) SVD simulated field, D) FEM-simulated field in the presence of T-shape as a scattering object, and E) FEM-simulation of the field in 3D. Note that for visualization purposes the pressure scale in E) does not start from zero and thus the pressures in A), C), and D) are not visible in E).

D. *Complex-shaped samples*

We performed experiments with three different letters, Fig. 1. The letters were made from foam clay and were 2 cm (>2 λ) in extent. Also, 3D printed polylactide (PLA) samples were levitated successfully but were less stable in the upright orientations since they were denser than the foam letters. Foam clay was selected as it is easy to mold into desired shapes and since it is light, 0.085 g/cm^3. The foam clay samples weighed 0.01 g and were 1 – 1.25 mm thick (caliber).

E. *Acoustic field measurements*

To compare the simulations and the physical fields, Fig. 2, we measured the amplitude and phase maps of different asymmetric multi-traps. The measurements were performed with a custom-made two-axis translation stage with a transducer and waveguide attached to it. To achieve strong fields with the traps at desired locations, each transducer's phase and amplitude was calibrated at the center of the levitator. Calibration was done by sending a continuous sine signal from one transducer at a time and by recording the amplitude and the phase shift of the received wave with the field measurement stage at center point.

III. Results and Discussion

Orientation and position of larger than 2λ-sized objects were controlled using several asymmetric acoustic traps. The samples were most stable when the asymmetric multi-trap was constructed from 3 to 4 individual asymmetric traps, depending on the levitated sample shape. For the T-shape we used four asymmetric traps, two around each of the straight parts, Fig. 2. The asymmetry parameter (α) in a single asymmetric trap was varied from 0.3 to 0.6, where α=0.3 indicates that the pressure gradient in the horizontal direction has an amplitude that is 30% of the pressure gradient in vertical direction (5).

The measured pressure field agrees with the numerically calculated one using (3) and the FEM-simulated fields as shown in Fig. 2. As seen in Fig. 2 E), the generated asymmetric traps act like acoustic tweezers holding the object against gravity and stably locking its orientation by wrapping around from the sides (blue pressure iso-surface).

The method allows rotating the larger-than-wavelength samples along all rotation axes; pitch, yaw, and roll, Fig. 3. The levitation is more stable when parts are aligned more in the horizontal plane than upright, as the acoustic pressure can support them directly against the gravity. Nonetheless, some shapes could be levitated also in upright orientation, Fig. 3 b). In the upright position, the vertical part appears to affect only the stability, while the levitation is a result of the pressure field acting on the horizontal part of the shape.

Sample translation was achieved along the x-, y-, and z-axes, Fig. 3 c). The maximum translation distance was 3 cm from the calibration point. Since the transducers phase offset was calibrated at one location (0,0,0), the phase offset at any other location (x, y, z) can be calculated by adding an additional geometric term to the calibrated phase $ik(\boldsymbol{r}_n + \boldsymbol{r}_1)$ (see (3) and Fig. 4). The accuracy of the transducers' coordinates directly translate into phase error. Thus, the levitation becomes less stable further away from the calibration point. To compensate for the inaccuracy in transducers locations, our next step is to apply calibration made in a 3D grid and thus estimate phase and amplitude more accurately.

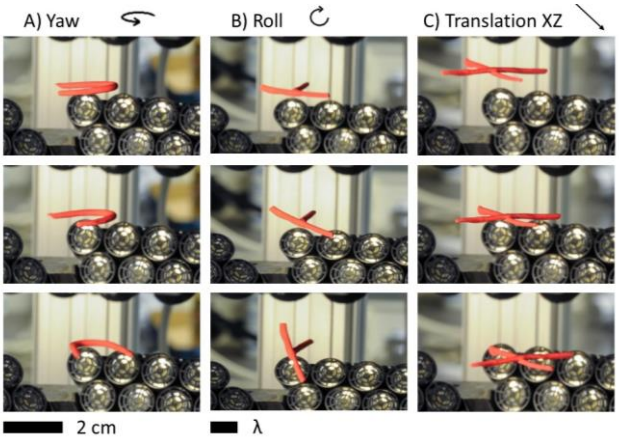

Fig. 3. A) U-shaped sample is rotated along the z-axis, B) T-shaped sample is rotated around the y-axis, and C) X-shaped object is translated simultaneously along x- and z-axes.

IV. Conclusions

We presented a method for controlled levitation of larger-than-wavelength complex-shaped samples, that comprise smaller than ¼ λ parts that fit inside the individual acoustic traps, e.g., letters. The samples can be manipulated in six degrees of freedom and in any combination of thereof.

To achieve stable orientation lock, the pressure field was tailored to a certain shape with multiple asymmetric traps. The acoustic multi-traps can be investigated numerically in an efficient manner, as the numerical calculations agree with the experimentally measured fields and FEM-models. The use of asymmetric multi-traps extends the diversity of samples that can be levitated and therefore generates new potential applications for acoustic levitation.

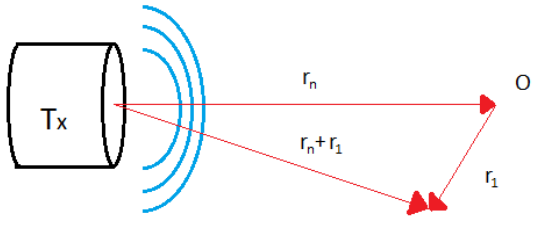

Fig. 4. Schematic illustration when a levitation trap is produced elsewhere than at the calibration point (0,0,0). Here $\boldsymbol{r}_n$ is the vector from the transducer to the calibration location and $\boldsymbol{r}_1$ is the vector from the center to the new desired spot.

REFERENCES

[1] A. Marzo, A. Seah S, B. W. Drinkwater, D. R. Sahoo, B. Long and S. Subramanian, "Holographic acoustic elements for manipulation of levitated objects," *Nat. Commun.*, No. 6,8661, 2015.

[2] E. Brandt, ”Suspended by sound,” *Nature*, pp. 474-475, 2001.

[3] L. Cox, A. Croxford, B. W. Drinkwater ja A. Marzo, ”Acoustic Lock: Position and orientation trapping of non-spherical sub-wavelength particles in midair using single-axis acoustic levitator,” *Appl. Phys. Lett.*, No. 113,054101, 2018.

[4] P. Helander, T. Puranen, A. Meriläinen, G. Maconi, A. Penttilä, M. Gritsevich, I. Kassamakov, A. Salmi, K. Muinonen ja E. Hæggström, ”Omnidirectional microscopy by ultrasonic sample control,” *Appl. Phys. Lett.*, No. 116,194101, 2020.

[5] V. Vandaele, P. Lambert ja A. Delchambre, ”Non-contact handling in microassembly: Acoustical levitation,” *Precis Eng*, vol. 29, No. 4, pp. 491-505, 2020.

[6] M. Andrade, A. ,. L. Bernassau ja J. Adamowski, ”Acoustic levitation of a large solid sphere,” *Appl. Phys. Lett.*, No. 109,044101, 2016.

[7] T. Puranen, P. Helander, A. Meriläinen, G. Maconi, A. Penttilä, M. Gritsevich, I. Kassamakov, A. Salmi, K. Muinonen ja E. Haeggström, ”Multifrequency Acoustic Levitation,” tekijä: *IEEE Int. Ultrason. Symp.*, Glasgow, United-Kindom, 2019.

[8] S. Zehnter, M. Andrade ja C. Ament, ”Acoustic levitation of a Mie sphere using a 2D transducer array,” *J. Appl. Phys.*, No. 129, 134901, 2021.

[9] L. ,. P. Gor'kov, ”On the forces acting on a small particle in an acoustical field in an ideal fluid,” Sov. Phys. Dokl., 1962.

[10] O. Sapozhnikov ja M. Bailey, ”Radiation force of an arbitrary acoustic beam on an elastic,” *J. Acoust. Soc. Am.*, pp. 661-676, 2013.

[11] M. Andrade, N. Pérez ja C. Adamowski J, ”Review of Progress in Acoustic Levitation,” *Brazilian J. Phys.*, No. 48, pp. 190-213, 2018.